LETTERS
PUBLISHED ONLINE: 23 AUGUST 2009 | DOI: 10.1038/NPHOTON.2009.142
nature photonics

Optical cleaning of congruent lithium niobate crystals

M. Kösters[1], B. Sturman[2], P. Werheit[1], D. Haertle[1] and K. Buse[1]*

Lithium niobate ($LiNbO_3$), also called the 'silicon of photonics', is indispensable in advanced photonics and nonlinear optics[1–10]. For many applications, however, the material is too polluted by transition metals, which are unavoidable at the parts per million level. These impurities serve as sources and traps for photoelectrons, causing optical damage and hampering the usability of $LiNbO_3$. Efforts have therefore been made to get rid of the photoexcitable electrons[11,12]. Here we introduce a method termed 'optical cleaning'. We show theoretically and experimentally that, if the material is heated to moderate temperatures, allowing ions to migrate and to maintain charge neutrality, an appropriately moving light beam pushes photoexcitable electrons out of the illuminated region like a brush, and provides exponential cleaning. This promises purification levels that are beyond the reach of current technologies.

Lithium niobate is a wide-gap ferroelectric material with a unique combination of physical properties, including ease of fabrication, robustness, transparency in the visible-to-infrared range, excellent electro-optic and nonlinear-optical characteristics, and the possibility to tailor ferroelectric domains[13,14]. It allows the realization of widely tunable and mirrorless optical parametrical oscillators[1,2], nonlinear whispering-gallery-mode resonators and modulators[3–5], nonlinear photonic crystals[6–8], non-reciprocal ultrafast laser writing[9], and optically gated persistent holographic recording[10]. Similar properties are inherent in $LiTaO_3$ crystals.

The main obstacle for the use of $LiNbO_3$ crystals in optics is optical damage—the deterioration of light beams as a result of the formation of unwanted refractive index changes[13,15,16]. Here, charge is separated owing to the bulk photovoltaic effect, leading to strong index changes by means of the linear electro-optic effect[17,18]. Remnant iron centres (Fe^{2+}/Fe^{3+}) are, most probably, responsible for this effect in undoped $LiNbO_3$ crystals, and the concentration of photo-excitable electrons is expected to be $\sim 1 \times 10^{15}$ cm^{-3}. Generally, other deep centres, including polarons and bipolarons[19–22], can also be photovoltaic. Considerable efforts have been made over the last decade to avoid optical damage[16]. The best method found to date—Mg doping—is costly and complicates domain engineering.

Here we introduce a method to achieve cleaning of such materials using light. Figure 1 illustrates the physical process. A light beam excites electrons and causes a photovoltaic current that originates from the polarity of the crystal[17,18]. The electrons are accordingly pushed along the polar c-axis, regardless of the type of photovoltaic centres. At room temperature this process stops quickly, because the electric field that arises blocks the photovoltaic current. However, heating of the crystals to moderate temperatures, $\sim$180 °C, mobilizes H^+ ions, which are present in many materials, or Li^+ ions. These ions drift and compensate the electronic space-charge field. This allows the light to continue to move electrons from the illuminated region along the c-axis. Although

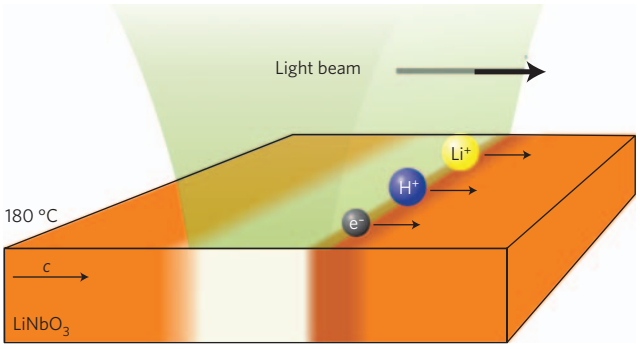

Figure 1 | Principle of optical cleaning. A light beam excites electrons from Fe^{2+} centres to the conduction band, pushes them in the c-direction, and provides efficient optical cleaning. Charge neutrality is maintained by mobile optically inactive ions. The colour profile of the crystal indicates the concentration pattern of photoexcitable electrons.

the arrangement described so far provides some cleaning[23], the light brush can be improved by one further trick: one has to move the light beam with just the right speed.

The described prerequisites for optical cleaning are similar to those for thermal fixing in $LiNbO_3$, producing persistent ionic gratings[16]. However, the scales and purposes of these two effects and methods are entirely different. Furthermore, similarities to 'zone refining', which is used to purify metals and crystals, are obvious, although the underlying physical processes are different.

A few conventional equations form the physical background for the optical cleaning effect. Indeed, the electronic and ionic current densities are relevant:

$$j_e = -e\beta N_e I + e\mu_e\left(n_e E + \frac{k_B T}{e}\frac{\partial n_e}{\partial z}\right), \quad j_i = e\mu_i N_i E \qquad (1)$$

Here, e is the elementary charge, β is the photovoltaic coefficient, $N_{e,i}$ are the densities of photoexcitable electrons and mobile ions, I is the light intensity, $\mu_{e,i}$ are the electronic and ionic mobilities, E is the electric field, k_B is Boltzmann's constant, T is the temperature, z is the coordinate along the c-axis, $n_e = sN_e I\tau_e/\hbar\omega$ is the density of photoexcited electrons, s is the absorption cross-section, $\hbar\omega$ is the light-quantum energy, and τ_e is the lifetime of photoexcited electrons. Thermal excitation of electrons is negligible for $T < 200$ °C (ref. 24). The terms entering j_e account for photovoltaic, drift and diffusion currents. Equations (1) have to be supplemented by the standard continuity and Poisson equations for $N_{e,i}$ and E. The initial concentrations $N^0_{e,i}$ are assumed to be spatially uniform. Sufficiently large values of $\mu_i N_i$ ensure an efficient ionic charge

[1]Institute of Physics, University of Bonn, Wegelerstr. 8, D-53115 Bonn, Germany, [2]Institute of Automation and Electrometry, Koptyug Ave. 1, 630090 Novosibirsk, Russia. *e-mail: kbuse@uni-bonn.de

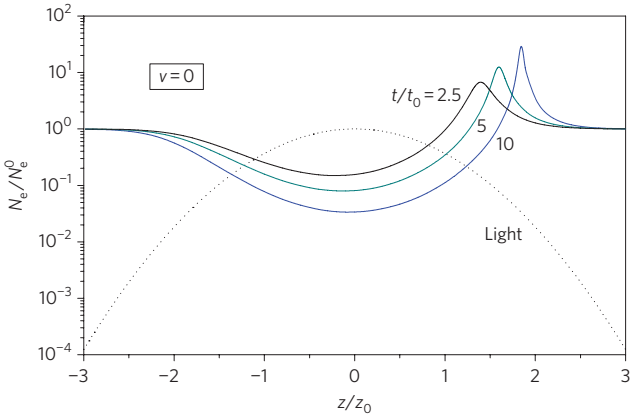

Figure 2 | Optical cleaning with a static light beam. The density N_e of photoexcitable electrons (normalized to N_e^0) is shown versus the coordinate for different cleaning times t. Pronounced cleaning at the beam centre is obvious.

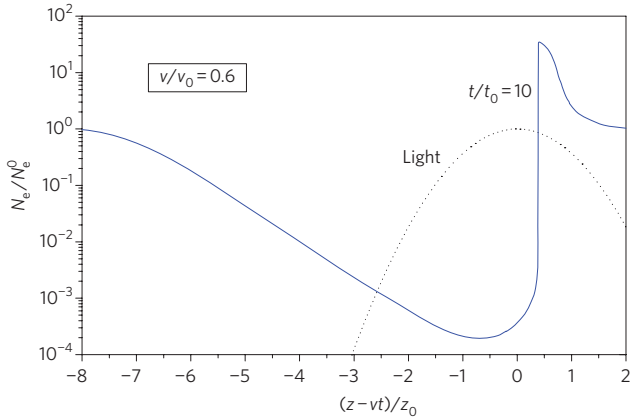

Figure 3 | Optical cleaning with a moving light beam. The density of photoexcitable electrons N_e (normalized to N_e^0) is shown versus the coordinate for a cleaning time $t = 10t_0$ and a beam velocity $v = 0.6v_0$. Excellent cleaning within a wide area is evident.

compensation, as it is needed for the photovoltaically driven cleaning process.

For simplicity, we consider a Gaussian cleaning light beam,

$$I = I_0 \exp\left[-(z - vt)^2/z_0^2\right] \qquad (2)$$

where I_0 is the peak intensity, v is the beam velocity, t is the time, and z_0 is the $1/e$ half-width.

Now we turn to predictions of the model for the concentration profile $N_e(z,t)$. Direct numerical simulations of the equations verify and supplement available analytical solutions that rely on the use of the method of characteristics[25] and have strong links with nonlinear dynamics[26].

Figure 2 shows the cleaning performance for a static light beam, $v = 0$. The photoexcitable electrons are pushed to one side of the illuminated region where they accumulate. The central part is cleaned: for the parameters used, the electron concentration is reduced by a factor of up to 75. The cleaning time is normalized to the characteristic photovoltaic drift time $t_0 = z_0/\beta I_0$, which does not depend on N_e^0. The blocking effect of a space-charge field is neglected, which means fulfilment of the inequalities $N_e^0 \ll N_i^0$ and $\mu_e n_e^0 \ll \mu_i N_i^0$, where $n_e^0 = sN_e^0 I_0 \tau_e/\hbar\omega$.

A dramatic enhancement of the cleaning performance occurs for a moving light brush, as shown in Fig. 3. For $t/t_0 \approx 10$ we already achieve a reduction of four orders of magnitude in N_e. The beam velocity v is set to $0.6v_0$, where $v_0 = \beta I_0$ is the photovoltaic drift velocity. The other relevant figures for the presented numerical example are $N_e^0/N_i^0 = 0.01$ and $\mu_e n_e^0/\mu_i N_i^0 = 0.01$. As long as these ratios remain small, their variations affect only secondary details of the optical cleaning.

An analytical treatment, confirmed by direct numerical simulations, gives a remarkable result:

$$N_e^{\min}(t)/N_e^0 = \exp(-\gamma t/t_0) \qquad (3)$$

where the position of the minimum concentration in the moving coordinate frame is given by $(z - vt)_{\min} = -z_0\sqrt{\ln(v_0/v)}$. The increment $\gamma(v/v_0) = (2v/v_0)\sqrt{\ln(v_0/v)}$ has a maximum $\gamma_{\max} \simeq 0.86$ at $v/v_0 \simeq 0.6$. Exponential cleaning, which shows neither saturation nor slowing down in time, is thus possible, promising purity levels far beyond the current state of the art. This feature is deeply inherent in photovoltaic charge transport.

To reliably suppress optical damage, the concentration of photoexcitable electrons in undoped crystals must be reduced from $\sim 1 \times 10^{15}$ to $\sim 1 \times 10^{11}$ cm^{-3}. This reduction ensures a charge limitation that is sufficient to suppress optical damage. Efficient optical cleaning requires an appropriate choice of the experimental parameters z_0, I_0 and v, and knowledge of the material parameters, particularly the concentration N_i^0. Such an optimization is not a trivial task.

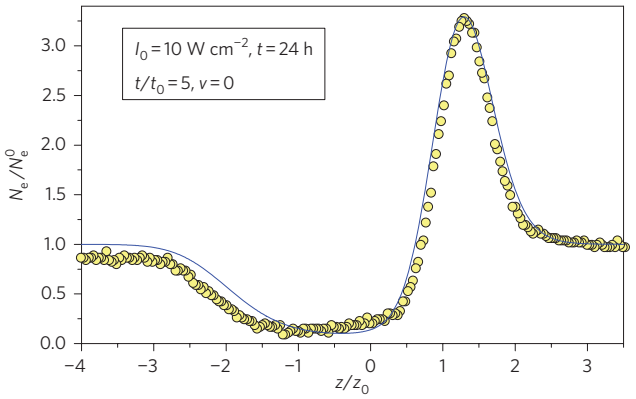

Figure 4 | Concentration profiles showing experimental and simulated results. Normalized profile N_e/N_e^0 versus the coordinate (open circles). The solid theoretical line corresponds to $t/t_0 = 5$.

The main goal of our first experiments is a proof of the principle. Monitoring of the profile $N_e(z)$ is possible only in doped $LiNbO_3$ crystals with $N_e^0 \gtrsim 1 \times 10^{17}$ cm^{-3}, showing measurable absorption. Thus we use congruent $LiNbO_3$ crystals doped with 0.01 mol% Fe.

First, we use an Ar^+ laser. The beam with $I_0 \simeq 10$ W cm^{-2} is static, and the cleaning duration is $t \simeq 5t_0 \simeq 24$ h. The resulting profile $N_e(z)$ is well resolved (Fig. 4). A 10-fold reduction of N_e is achieved. The solid line represents our simulation, showing good agreement with the experiment. Note that the simulation includes the convolution of the true profile $\rho(z)$ and the Gaussian profile of the test beam; this smoothes the peak and decreases $N_e^{\max}$ by ~40%.

Next, we used more challenging cleaning parameters with a Nd:YAG laser: $t \simeq 340$ h, $I_0 \simeq 15$ W cm^{-2} and $v \simeq 3 \times 10^{-3}$ mm h^{-1}, which correspond to $t/t_0 \approx 1 \times 10^2$ and $v/v_0 \approx 1 \times 10^{-1}$. After the treatment, we were unable to see light absorption in the cleaned (~1 mm wide) region. The ratio N_e/N_e^0 had certainly become smaller than 0.05. At the same time, we detected a strong suppression of optical damage in the cleaned area, with an increase in the

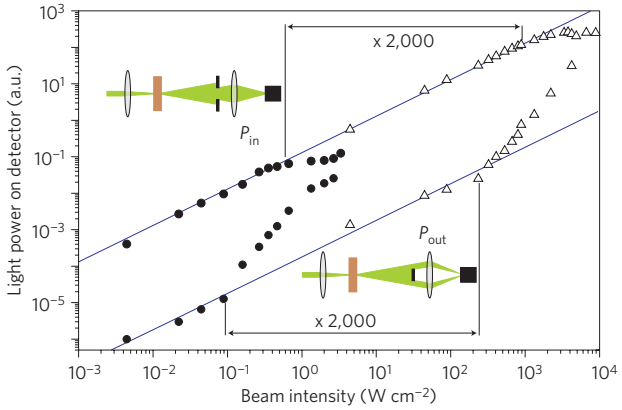

Figure 5 | Evidence for optical damage suppression. Intensity dependence of the light powers P_{in} and P_{out} for the cleaned (triangles) and uncleaned (circles) areas versus the intensity of a beam inducing optical damage. Deviation from the linear dependence indicates the threshold of optical damage. The insets illustrate the geometry of the purification measurements.

threshold of optical damage of more than three orders of magnitude. This is shown in Fig. 5.

In addition, the first attempts at optical cleaning of nominally undoped crystals were made. With non-optimized parameters we achieved a factor-of-five enhancement of the optical damage threshold.

The cleaning efficiency is controlled by four variable parameters: light intensity, beam size, moving speed of the beam and temperature. It depends also on the background concentrations of electrons and compensating ions. Optimization of the parameters of optical cleaning for nominally undoped crystals is challenging because absorption and photoconductivity become too small to be measured directly[27].

Some further issues are worth highlighting. Optical cleaning represents a new effect in which the density of photoexcitable electrons in polar crystals can be reduced by orders of magnitude, strongly changing the optical properties. To estimate practicability, the speed of optical cleaning is at first glance an issue. However, one has to consider that optical cleaning of undoped material can be much faster. Also, cleaning is needed just once during the crystal life. Furthermore, cheap high-power light-emitting diodes could also clean crystals. Many cleaning stations could thus be used in parallel, providing a high material throughput.

Compared to the recently proposed thermo-electrical cleaning[11,12], optical cleaning is a more gentle treatment. In particular, stoichiometry is not changed because of the lower temperatures used. Furthermore, the optical process provides a stronger and more controlled cleaning.

In conclusion, we have shown that a long-term exposure of $LiNbO_3$ crystals at elevated temperatures leads to a strong reduction in the concentration of photoexcitable electrons by means of the photovoltaic charge transport. Using a properly matched moving light beam strongly enhances the cleaning rate. A reduction of the electron concentration by several orders of magnitude is found to be attainable and sufficient to strongly suppress the optical damage. Because no special assumptions on $LiNbO_3$ crystals were used, the cleaning method is applicable to numerous optical materials of pyro- and piezoelectric symmetry showing the bulk photovoltaic effect.

Methods

Realizing optical cleaning. For most of the experiments we used congruent $LiNbO_3$ crystals doped with 0.01 mol% Fe and with the dimensions $x \times y \times z = 1 \times 4 \times 5$ mm^3, with $N_e^0 \simeq 6 \times 10^{16}$ cm^{-3} known from absorption spectroscopy[28]. The initial H^+ concentration, deduced from absorption measurements at 2,870 nm (ref. 29), was $\sim 2 \times 10^{18}$ cm^{-3}. For the cleaning step, we used light beams at 514 or 532 nm from Ar^+ or Nd:YAG lasers. Each beam was expanded and then focused onto the y,z-face using a cylindrical lens with a focal length of 70 cm. The Gaussian widths z_0 used were $\sim$70 and 42 μm. The temperature was kept at 180 °C during the cleaning process. After cooling to room temperature, inspection of the light absorption was performed using a weak light beam at 543 nm with a $1/e$-radius of 35 μm provided by a HeNe laser. Moving the crystal yielded a scan of the absorption profile and hence provided the profile $N_e(z)$.

For experiments on optical cleaning of nominally undoped crystals a light beam from the Nd:YAG laser was focused to obtain a Gaussian width z_0 of 20 μm. This gave a peak intensity $I_0 = 1{,}000$ W cm^{-2}. During the 39 h cleaning treatment the light beam was moved 325 μm, equal to a moving speed of $\sim 8 \times 10^{-3}$ mm h^{-1}.

Purification measurements. A focused beam ($1/e$-radius of 20 μm) at 514 nm from an Ar^+ laser was directed onto the sample. After a 150-s exposure with intensities in the range $1 \times 10^{-3} - 1 \times 10^4$ W cm^{-2}, the output beam divergence was measured in two ways. First, a pinhole behind the sample blocked the stray light, and a photodiode was used to record the power P_{in} (ref. 30). Second, a microdisk blocked the beam centre, so that the power P_{out} was recorded. Both measurement schemes are sketched in Fig. 5. The onset of optical damage yielded a decrease in P_{in} and an increase in P_{out}.

Received 7 April 2009; accepted 23 July 2009; published online 23 August 2009

References

1. Dunn, M. H. & Ebrahimzadeh, M. Parametric generation of tunable light from continuous-wave to femtosecond pulses. *Science* **286,** 1513–1517 (1999).
2. Canalias, C. & Pasiskevicius, V. Mirrorless optical parametric oscillator. *Nature Photon.* **1,** 459–462 (2007).
3. Ilchenko, V. S., Savchenkov, A. A., Matsko, A. B. & Maleki, L. Nonlinear optics and crystalline whispering gallery mode cavities. *Phys. Rev. Lett.* **92,** 043903 (2004).
4. Guarino, A., Poberaj, G., Rezzonico, D., Degl'Innocenti, R. & Günter, P. Electro-optically tunable microring resonators in lithium niobate. *Nature Photon.* **1,** 407–410 (2007).
5. Hsu, R. C. J., Ayazi, A., Houshmand, B. & Jalali, B. All-dielectric photonic-assisted radio front-end technology. *Nature Photon.* **1,** 535–538 (2007).
6. Zhu, S., Zhu, Y. & Ming, N. Quasi-phase-matched third-harmonic generation in a quasi-periodic optical superlattice. *Science* **278,** 843–846 (1997).
7. Broderick, N. G. R., Ross, G. W., Offerhaus, H. L., Richardson, D. J. & Hanna, D. C. Hexagonally poled lithium niobate: a two-dimensional nonlinear photonic crystal. *Phys. Rev. Lett.* **84,** 4345–4348 (2000).
8. Soljacic, M. & Joannopoulos, J. D. Enhancement of nonlinear effects using photonic crystals. *Nature Mater.* **3,** 211–219 (2004).
9. Yang, W., Kazansky, P. G. & Svirko, Y. P. Non-reciprocal ultrafast laser writing. *Nature Photon.* **2,** 99–104 (2008).
10. Buse, K., Adibi, A. & Psaltis, D. Non-volatile holographic storage in doubly doped lithium niobate crystals. *Nature* **393,** 665–668 (1998).
11. Falk, M. & Buse, K. Thermo-electric method for nearly complete oxidization of highly iron-doped lithium niobate crystals. *Appl. Phys. B* **81,** 853–855 (2005).
12. Gronenborn, S., Sturman, B., Falk, M., Haertle, D. & Buse, K. Ultraslow shock waves of electron density in $LiNbO_3$ crystals. *Phys. Rev. Lett.* **101,** 116601 (2008).
13. Kuz'minov, Y. S. *Lithium Niobate Crystals* (Cambridge Univ. Press, 1999).
14. Myers, L. E., Eckardt, R. C., Fejer, M. M. & Byer, R. L. Quasi-phase-matched optical parametric oscillators in bulk periodically poled $LiNbO_3$. *J. Opt. Soc. Am. A* **12,** 2102–2116 (1995).
15. Solymar, L., Webb, D. & Grunnet-Jepsen, A. *The Physics and Applications of Photorefractive Materials* (Clarendon Press, 1996).
16. *Photorefractive Materials and Their Applications I, II* (eds Günter, P. & Huignard, J.-P.) (Springer, 2006, 2007).
17. Glass, A. M., von der Linde, D. & Negran, T. J. High-voltage bulk photovoltaic effect and the photorefractive process in $LiNbO_3$. *Appl. Phys. Lett.* **25,** 233–235 (1974).
18. Fridkin, V. & Sturman, B. *The Photovoltaic and Photorefractive Effects in Noncentrosymmetric Materials* (Gordon & Breach, 1992).
19. Maleki, L. & Matsko, A. *Ferroelectric crystals for photonic applications*, 337–383 (Springer, 2008).
20. Schirmer, O. F., Imlau, M., Merschjann, C. & Schoke, B. Topical review: electron small polarons and bipolarons in $LiNbO_3$. *J. Phys.: Condens. Matter* **21,** 123201 (2009).
21. Jermann, F. & Otten, J. Light-induced charge transport in $LiNbO_3$:Fe at high light intensities. *J. Opt. Soc. Am. B* **10,** 2085–2092 (1993).
22. Yan, W. B. *et al.* Influence of composition on the photorefractive centers in pure $LiNbO_3$ at low light intensity. *Appl. Opt.* **45,** 2453–2458 (2006).
23. Becker, R. A. 'Thermal fixing' of Ti-indiffused $LiNbO_3$ channel waveguides for reduced photorefractive susceptibility. *Appl. Phys. Lett.* **45,** 121–123 (1984).

24. Sturman, B. I., Carrascosa, M., Agulló-López, F. & Limeres, J. Two kinetic regimes for high-temperature photorefractive phenomena in $LiNbO_3$. *J. Opt. Soc. Am. B* **15,** 148–151 (1998).
25. Jeffrey, A. *Handbook of Mathematical Formulas and Integrals* (Academic Press, 2004).
26. Whitham, G. B. *Linear and Nonlinear Waves* (Wiley-Interscience, 1974).
27. Jermann, F., Simon, M. & Krätzig, E. Photorefractive properties of congruent and stoichiometric lithium niobate at high light intensities. *J. Opt. Soc. Am. B* **12,** 2066–2070 (1995).
28. Kurz, H. *et al.* Photorefractive centers in $LiNbO_3$, studied by optical-, Mössbauer- and EPR-methods. *Appl. Phys.* **12,** 355–368 (1977).
29. Klauer, S., Wöhlecke, M. & Kapphan, S. Influence of H-D isotopic substitution on the protonic conductivity of $LiNbO_3$. *Phys. Rev. B* **45,** 2786–2799 (1992).
30. Rams, J., Alcázar-de-Velasco, A., Carrascosa, M., Cabrera, J. M. & Agulló-López, F. Optical damage inhibition and thresholding effects in lithium niobate above room temperature. *Opt. Commun.* **178,** 211–216 (2000).

Acknowledgements

The authors thank M. Falk for useful discussions, and the Deutsche Forschungsgemeinschaft (Research Unit 557) and the Deutsche Telekom AG for financial support.

Author contributions

The project was planned by K.B., M.K. and D.H. The experiments were performed by M.K. and P.W. Data were analysed by B.S., M.K., P.W., D.H. and K.B.

Additional information

The authors declare competing financial interests: details accompany the full-text HTML version of the paper at www.nature.com/naturephotonics. Reprints and permission information is available online at http://npg.nature.com/reprintsandpermissions/. Correspondence and requests for materials should be addressed to K.B.